Journal of Power Sources 195 (2010) 5686–5691

Contents lists available at ScienceDirect

Journal of Power Sources

journal homepage: www.elsevier.com/locate/jpowsour

Surface modification and performance of inexpensive Fe-based bipolar plates for proton exchange membrane fuel cells

Ching-Yuan Bai[a,b,*], Tse-Min Wen[c], Mao-Suan Huang[b,d], Kung-Hsu Hou[e,**], Ming-Der Ger[a], Shuo-Jen Lee[f]

[a] Department of Applied Chemistry & Materials Science, National Defence University, Chung Cheng Institute of Technology, No. 190, Sanyuan 1st St., Tahsi, Tau-Yuan 335, Taiwan, ROC
[b] Research Center for Biomedical Devices, Taipei Medical University, Taipei 110, Taiwan
[c] School of Defense Science, National Defense University, Chung Cheng Institute of Technology, Tao-Yuan, Taiwan, ROC
[d] Department of Dentistry, Taipei Medical University-Shuang Ho Hospital, Taipei 235, Taiwan
[e] Department of Power Vehicle and System Engineering, National Defense University, Chung Cheng Institute of Technology, No. 190, Sanyuan 1st St., Tahsi, Tao-Yuan 335, Taiwan, ROC
[f] Fuel Cell Center, Yuan-Ze University, Tao-Yuan, Taiwan, ROC

ARTICLE INFO

Article history:
Received 12 March 2010
Accepted 12 March 2010
Available online 19 March 2010

Keywords:
Fe-based alloys
Rolling
Bipolar plates
Low-temperature pack chromization

ABSTRACT

A reforming pack chromization with rolling pretreatment process is utilized to develop inexpensive and high-performance Fe-based metal bipolar plates (SS 420, SS 430, and SS 316 stainless steels) for PEMFC systems. Rolling process is previously performed to reduce the chromizing temperature and generate a coating possessing excellent conductivity and corrosion resistance on the steels during chromization. The power efficiencies of rolled-chromized and simple chromized bipolar plates are compared with graphite bipolar plates employed in PEMFCs. The results show that the rolled-chromized bipolar plates have a corrosion current (I_{corr}) of 7.87×10^{-8} A cm^{-2} and an interfacial contact resistance of 9.7 mΩ cm^2. Moreover, the power density of the single cell assembled with rolled-chromized bipolar plates is 0.46 W cm^{-2}, which is very close to that of graphite (0.50 W cm^{-2}), in the tested conditions of this study.

1. Introduction

Plenty energy consumption have caused the serious issues of global warming and energy crisis and attracted a great deal of attention in the world wild. Many countries have made a lot of efforts to develop new alternative energy and technology. The fuel cell is quiet, clean, and efficient energy conversion method for portable applications, thus offers a promising technology for renewable power sources. Among diverse fuel cells, proton electrolyte membrane fuel cells (PEMFCs) possess many advantages such as light-weight, compactness, high power efficiency, and operation at low temperatures [1,2]. The requirements of bipolar plates characteristics are higher electric conductivity, corrosion resistance, mechanical strength, gas impermeability, and lower mass and cost. Nowadays, graphite has been used as the material of bipolar plates owing to its chemical nobility and high electrical conductivity. The high cost for manufacturing flow-field patterns on graphite sheets and the brittleness of graphite are the major troubles in using this material for the widespread marketplace. Moreover, the graphite bipolar plate account for the large percent of mass and volume in a PEMFC. Recently, the employment of metallic bipolar plates has received attention due to the ease to fabricate and superior mechanical properties of metals allowing designs of a smaller and thinner stack to reduce the weight and volume of fuel cells. However, performance and lifetime of the presented metallic bipolar plates do not meet the demand currently [3,4].

Metal alloys could easily be introduced into the bipolar plate process due to their extensible property and the low cost of fabrication. However, the main obstacle of metals is the lack of ability to prevent corrosion in the harsh acidic and humid environment inside the PEM fuel cell without coatings and passive layers. For that reason, metal ions dissolved from the metallic bipolar plates will cause considerable power degradation of fuel cell [5]. Although noble metals, such as gold and platinum, are generally with excellent corrosion resistance, the high price prevents these materials from being used. Stainless steels and titanium alloys are other desirable materials. However, the main challenge is that these metal bipolar plates develop a passivating oxide layer on the surface, which protect the bulk metal from progression of corrosion but cause an undesirable effect of a high surface contact resistance. At present, many surface modifications on diverse stainless steels have been published [6–10].

* Corresponding author. Tel.: +886 3 3891716; fax: +886 3 3892494.
** Co-corresponding author. Tel.: +886 3 3800969; fax: +886 3 3895570.
E-mail addresses: cybai@ccit.edu.tw (C.-Y. Bai), khou@ccit.edi.tw (K.-H. Hou).

0378-7753/$ – see front matter © 2010 Elsevier B.V. All rights reserved.
doi:10.1016/j.jpowsour.2010.03.048

Table 1
Specimen names and corresponding conditions.

Specimen name	Substrate	Chromization temp. and duration
420-Cr(700-2)	420 stainless steel	700 °C, 2 h
420-R-Cr(700-2)	Rolled 420 steel	700 °C, 2 h
316-Cr(700-2)	316 stainless steel	700 °C, 2 h
316-R-Cr(700-2)	Rolled 316 steel	700 °C, 2 h
430-Cr(700-2)	316 stainless steel	700 °C, 2 h
430-R-Cr(700-2)	Rolled 430 steel	700 °C, 2 h

In this study, chromized stainless steels were chosen as the alternative bipolar plates for considering the requirement of bipolar plates in PEMFCs. SS 420, SS 430, and SS 316 stainless steels were used as the substrates to be coated a chromium-carbide based layer with low-temperature chromization processes. Then, the short-term and long-term performance of surface modified bipolar plates were investigated and discussed.

2. Experimental

2.1. Fabrication of metallic bipolar plates

In the previous investigation [11], the procedure of the low-temperature pack chromization effectively employed on the AISI 1045 carbon steel have been presented. SS 420, SS 430, and SS 316 stainless steels were chosen as substrates of bipolar plates in this study. The pack powder mixtures used to chromize the steels contained a master metal (Cr), an activator (NH_4Cl), and an inert filler (Al_2O_3). Various chromized coatings have been simply named, and the specimen names and corresponding conditions are shown in Table 1. Before pack chromization process, bipolar plates were rolled and then manufacturing flow-field patterns standing on schematic diagram shown as Fig. 1. Subsequently, chromized processes were carried out.

2.2. Electrochemical test

Potentiodynamic polarization tests were conducted with a three electrode potentiostat system to evaluate the electrochemical behavior of simple chromized and rolling-chromized steel sheets. A saturated calomel electrode (SCE) was used as a reference to measure the potential across the electrochemical interface. The tests were carried out by sweeping potential range from −0.5 V to 0.8 V with a scanning rate of 0.5 mV s^{-1} in a 0.5 M H_2SO_4 solution without purging any gases at room temperature. Before the tests, all specimens were degreased and rinsed with deionized water. Fresh corrosion bath was used for each new specimen.

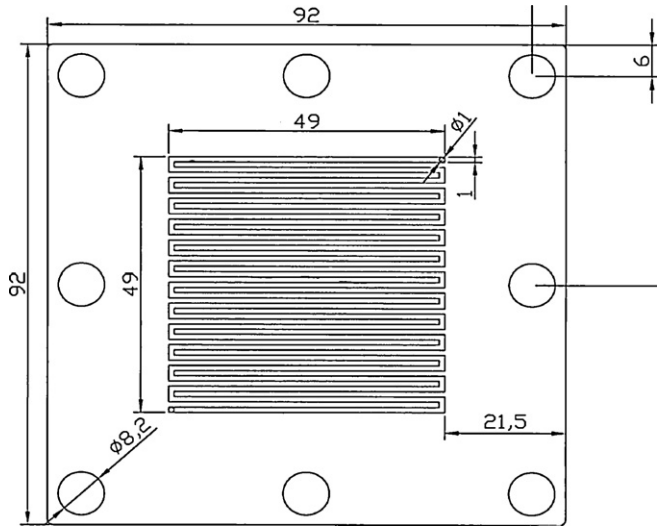

Fig. 1. The schematic diagram of chromized bipolar plates with flow-field patterns.

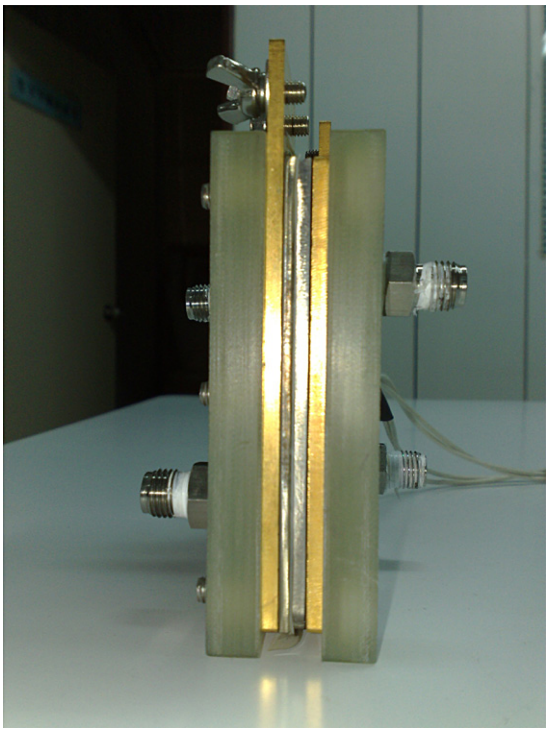

Fig. 2. The prototype of single cell stack with chromized bipolar plates.

2.3. Interfacial contact resistance (ICR) measurement

Measurement techniques for interfacial contact resistance had been well documented in previous literatures [12–14]. In this work, the interfacial contact resistance between the specimens and GDL (carbon paper) was evaluated by a method similar to the report by Wang et al. [14].

2.4. Fabrication of a single cell

The single PEM cells, fabricated with Fe-based metallic bipolar plates in this work, possess an active area of 25 cm^2. The membrane electrode assembly (MEA) consisted of Nafion 112 membranes and Torry paper with a catalyst loading of 0.2 mg cm^{-2} on anode and 0.4 mg cm^{-2} on cathode electrode. The silicone rubber film with 200 μm thickness was used as gasket to prevent gas leakage. The end plate were made of glasses fiber and machined to fabricate the gas ports and installation holes of cell. In addition, the Au electroplated copper plates were used as the current collector. Subsequently, every bolt was evenly loaded the compaction force of 20 kg to assemble the components mentioned above. The cell components were assembled in the order of an end plate, current collector, bipolar plate, gasket, MEA, gasket, bipolar plate, current collector, and end plate. The finished single PEM cell is shown in Fig. 2.

2.5. Single cell tests

Cell voltages and power densities as function of current density for the single cells were measured and plotted with *I–V* and *I–P* curves in the operation region of 0.9–0.35 V. The long-term performance test of the cell was conducted at operation voltage of 0.5 V for 100 h. The as-built single cell was operated at 50 °C under

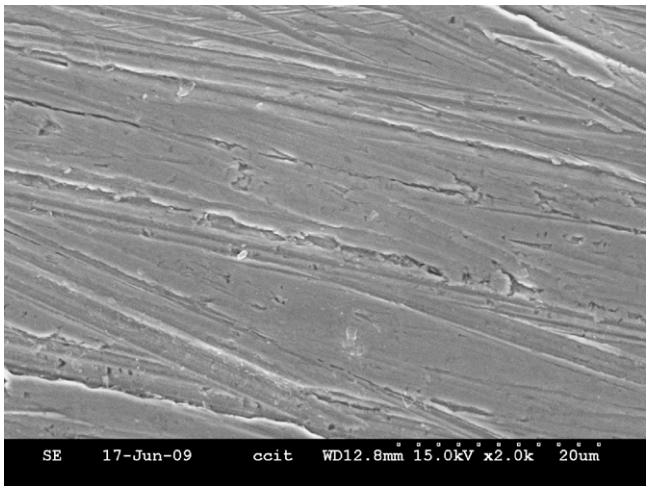

Fig. 3. The SEM surface image of bare SS 420 bipolar plates.

ambient pressure. Pure hydrogen and air which were fully humidified at 70 °C were used as reactant gases at the anode and cathode sides, respectively. The flow rate of anode and cathode gases (Q_A and Q_C) was controlled at 300 $cm^3\ min^{-1}$. Nitrogen was used to purge the cell from residue gases before the cell operation. Moreover, metallic ions dissociated from the bipolar plates in the water by-product and membrane electrode assembly were examined by an inductively coupled plasma-mass spectrometer (ICP-MS) and XPS, respectively.

3. Results and discussion

3.1. Characteristics of chromized specimens

Figs. 3 and 4 show the SEM surface images of bare SS 420 and 420-R-Cr(700-2) bipolar plates, respectively. It is obviously found that the scrape caused by polishing distributed on the surface of base metal. Nevertheless, these regular stripes were disappeared and instead of the chromized coating generated by low-temperature pack chromization. The polarization curves of bare steels and various chromized coatings measured in the simulated PEMFC environment were shown in Fig. 5. The corrosion current density of any Fe-based bipolar plates produced in this work was clearly reduced by chromization process. Additionally, the

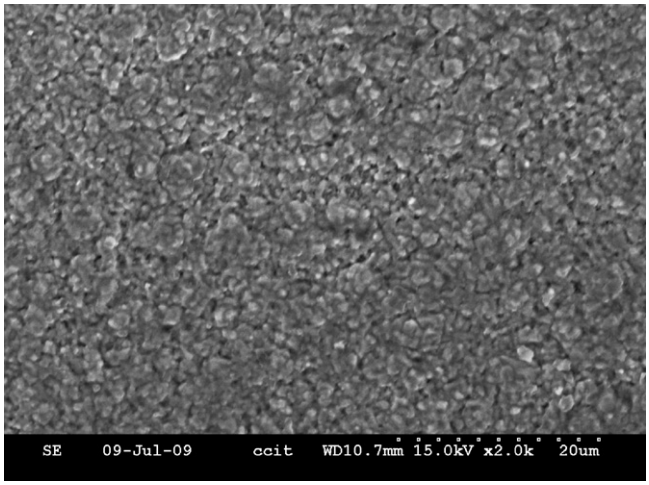

Fig. 4. The SEM surface image of 420-R-Cr(700-2) bipolar plates.

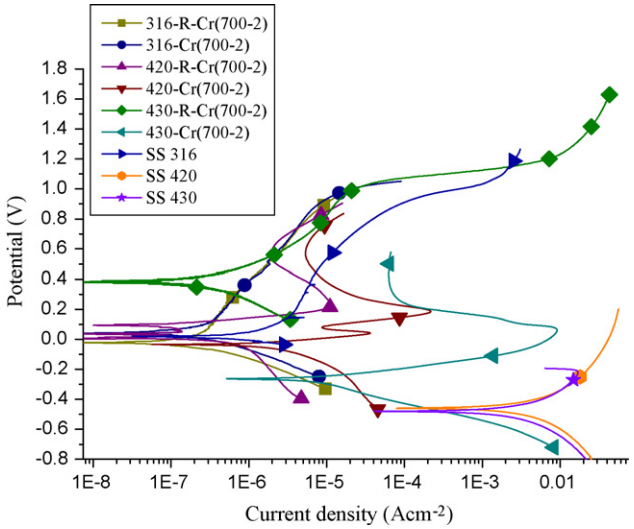

Fig. 5. Polarization curves of bare and various chromized steels measured in a 0.5 M H_2SO_4 solution at 25 °C.

chromized steels with rolling pretreatment exhibit better corrosion resistance than the simple chromized specimens for the same substrate. Therein, the corrosion current density of 316-R-Cr(700-2), 420-R-Cr(700-2) and 430-R-Cr(700-2) are 5.86×10^{-8}, 7.87×10^{-8} and 6.86×10^{-8} A cm^{-2}, respectively. The results of electrochemical tests showed that the corrosion resistance of these Fe-based steels can be enhanced significantly by the low-temperature pack chromization with rolling pretreatment.

The superficial compositions of 316-R-Cr(700-2), 420-R-Cr(700-2), and 430-R-Cr(700-2) specimens analyzed along a cross-sectional path by XPS techniques are shown in Fig. 6(a)–(c). As noted in the XPS depth profiles, although a small amount of oxides are produced in the superficial sites, the chromium carbides are the dominant compounds of all the chromized coatings. The Cr concentration of 420-R-Cr(700-2) specimen is higher than 60 at%, which is the highest among three rolled-chromized specimens. In addition, the average oxygen concentration (atomic percent) of the rolled-chromized coatings in the depth range of 0–300 nm beneath surface is shown in Table 2. Specifically, the oxygen concentration of 316-R-Cr(700-2) is higher than that of 420-R-Cr(700-2) as well as 430-R-Cr(700-2), revealing that the 316-R-Cr(700-2) coating possesses more oxides on the coatings. According to the literature published [15], Silva et al. indicated that the different amounts of chromium-oxide and ferrum-oxide on the surface can result in distinct conductivity. Moreover, it is well known that the conductivity of chromium-oxides is worse than that of chromium carbides. Hence, It could be expected that the conductivity of the 316-R-Cr(700-2) is lower than that of 420-R-Cr(700-2) and 430-R-Cr(700-2) specimens.

During operating a PEM fuel cell, the effect of the interfacial contact resistance between bipolar plates and gas diffusion layers on cell performance is more important than the resistance of bulk materials, since the resistance of the bulk materials is usually very small and can be neglected while compared with

Table 2
Average oxygen concentration of the coatings in the depth range of 0–300 nm beneath surface.

Specimens names	Oxygen concentration (at%)
316-R-Cr(700-2)	9.37
420-R-Cr(700-2)	4.43
430-R-Cr(700-2)	5.75

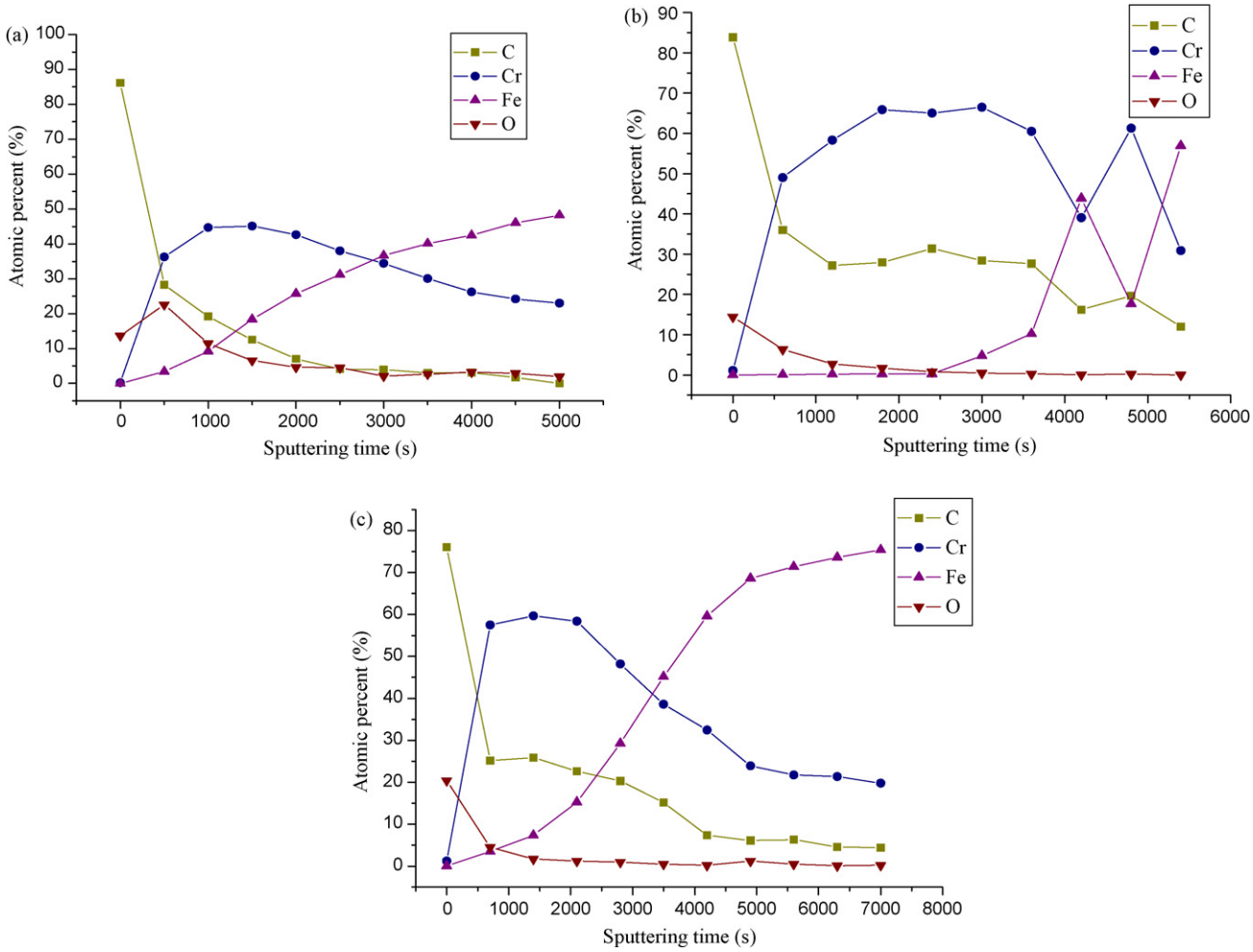

Fig. 6. XPS depth profiles of (a) 316-R-Cr(700-2), (b) 420-R-Cr(700-2), and (c) 430-R-Cr(700-2). The estimated sputtering rate was 1 Å s^{-1}.

the interfacial contact resistance. Fig. 7 shows the interfacial contact resistance curves of the bipolar plates, produced with bare and chromized steels, at various compaction pressures. It is clearly seen that the contact resistance of stainless steels with chromized coatings can be reduced significantly. In general, the chromized coatings on Fe-based steels are consisted mainly of chromium carbides, chromium nitrides, and a small amount of metal oxides [16]. A little of ferrum, which acts as a dopant to the carbide or nitride phase, results in many stoichiometry defects to increase the conductivity of the coatings. Hsu [17] indicated that the carbide of Cr_3C_2 with conductivity of $68 \times 10^6\ \Omega^{-1}\ cm^{-1}$ was used as conductive ceramics. In addition, the nitrides, produced by many methods on different substrates, exhibiting a good conductivity have been reported in the literatures [18–21]. Hence, the Fe-based steels with chromized coatings composed mainly of chromium carbides and chromium nitrides will possess higher conductivity than the bare steels with primarily chromium-oxides on the surface. Furthermore, the measurement results also show that the ranking of interfacial contact resistance of the chromized specimens, from greatest to least, is 316-Cr(700-2), 430-Cr(700-2), 316-R-Cr(700-2), 430-R-Cr(700-2), 420-Cr(700-2), and 420-R-Cr(700-2) at a given compaction pressure. Specifically, the contact resistance of 316-R-Cr(700-2), 430-R-Cr(700-2), and 420-R-Cr(700-2) are 11.6, 11.1, and 10.2 mΩ cm^2, respectively, at compaction pressure of 140 N cm^{-2}. Among all of testing bipolar plates, the 420-R-Cr(700-2) has the best conductivity owing to it possessing the highest concentration of chromium carbide and the lowest average concentration of oxides in the coatings. Obviously, the results of interfacial contact resistance measurements are in accordance with the XPS depth profiles stating in Fig. 6.

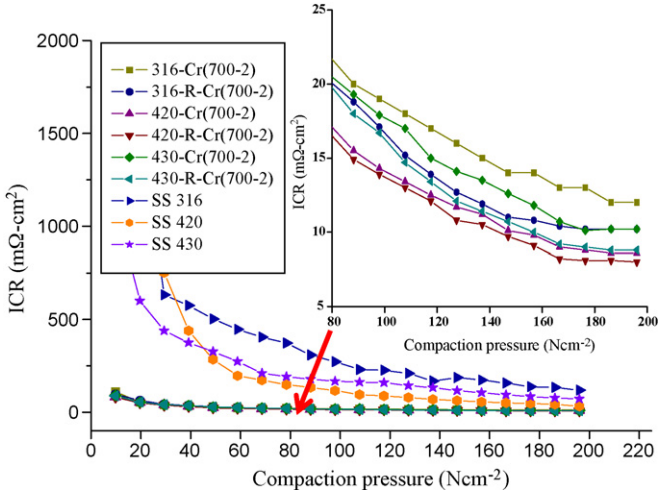

Fig. 7. Interfacial contact resistances between the bipolar plates and gas diffusion layer at various compaction pressures.

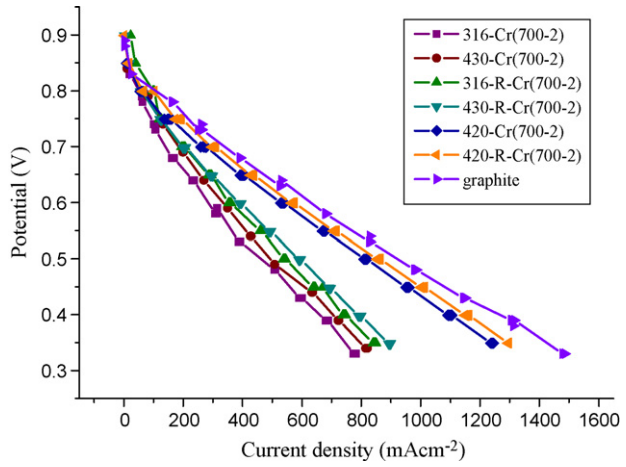

Fig. 8. *I–V* curves of the single cells assembled with the bare and various chromized steel bipolar plates; cell temperature = 50 °C; $Q_A = Q_C = 300\,cm^3\,min^{-1}$.

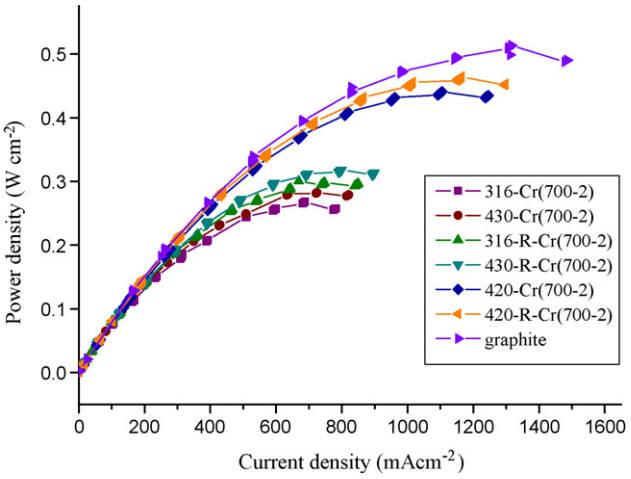

Fig. 9. *I–P* curves of the single cells assembled with the bare and various chromized steel bipolar plates; cell temperature = 50 °C; $Q_A = Q_C = 300\,cm^3\,min^{-1}$.

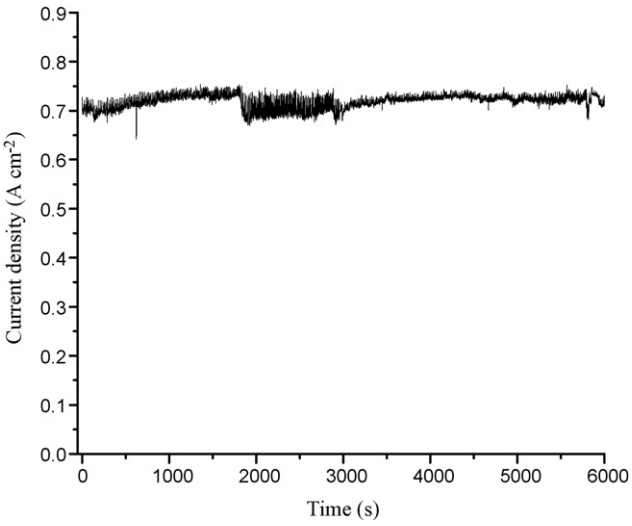

Fig. 10. Long-term performance of the single cell assembled with 420-R-Cr(700-2) bipolar plates measured at a cell voltage of 0.5 V; cell temperature = 50 °C; $Q_A = Q_C = 300\,cm^3\,min^{-1}$.

Table 3
The concentrations of metallic ions in the water produced from 420-R-Cr(700-2) bipolar plates after the cell testing.

Elements	Concentration (ppm)
Cr	0.11286
Fe	0.098
Ni	0.094

3.2. Single cell performance

The initial *I–V* curves of single cells assembled with the bare and various chromized steel bipolar plates are shown in Fig. 8. The results show that the open circuit voltage (OCV) of the cells fabricated with 420-R-Cr(700-2), 420-Cr(700-2), 430-R-Cr(700-2), 316-R-Cr(700-2), 316-Cr(700-2), and 430-Cr(700-2) are 0.9 V, 0.88 V, 0.9 V, 0.9 V, 0.85 V and 0.85 V, respectively, and the voltage or

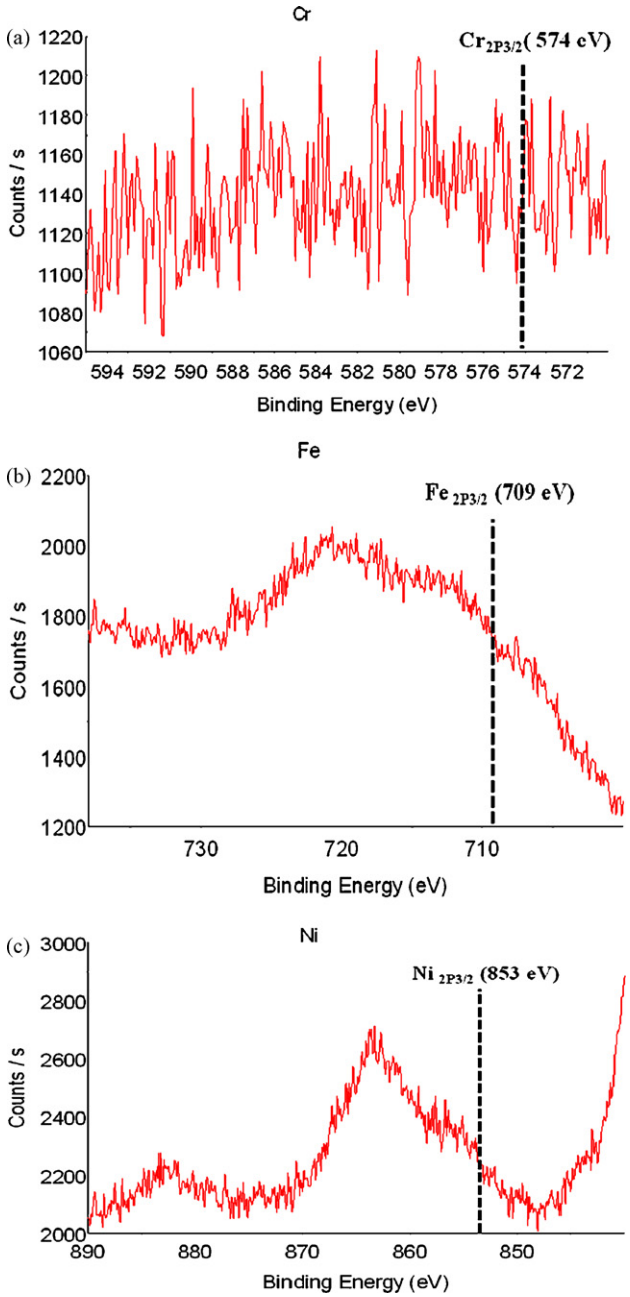

Fig. 11. The binding energy profiles of (a) Cr, (b) Fe, and (c) Ni on the surface of membrane electrode assembly after the single cell operation for 100 h.

performance of the single cells at low current densities are almost equivalent. At a cell voltage of 0.6 V, the current density of the single cells assembled with 316-Cr(700-2), 430-Cr(700-2), 316-R-Cr(700-2), 430-R-Cr(700-2), 420-Cr(700-2), and 420-R-Cr(700-2) bipolar plates are 313.6, 349.2, 361.2, 395.6, 540.4, and 573.2 mA cm^{-2}, respectively, which is coincident with the opposite trend of interfacial contact resistances in Fig. 7. Therefore, it is speculated that the interfacial contact resistance of the cells fabricated with metallic bipolar plates is the dominated factor to affect the performance of PEM fuel cells. The initial *I–P* curves of single cells assembled with the bare and chromized steel bipolar plates are shown in Fig. 9. The single cells assembled with 420-R-Cr(700-2) bipolar plates possess the highest power density (0.46 W cm^{-2}) among all of the chromized steel bipolar plates, which is very close to that of the cell with graphite bipolar plates (0.50 W cm^{-2}) in the testing conditions of this work.

In order to evaluate the long-term performance of single cells fabricated with chromized steel bipolar plates, a long-term testing of the cell with 420-R-Cr(700-2) bipolar plates, which possess the best initial performance, was carried out for 100 h. The current density at a cell voltage of 0.5 V was plotted as a function of operation time in Fig. 10. During the operation of 100 h, the current density of the cell with 420-R-Cr(700-2) bipolar plates was maintained in the range of 0.68–0.73 A cm^{-2}, indicating that the cell is operating without performance degradation. Specifically, the fluctuating phenomenon was apparently presented in the performance testing curve, since the water produced by the cathode reaction accumulated temporarily on the flow field, but was removed quickly by the inlet gases. Furthermore, the corrosion products of bipolar plates can be a great source of ions for contamination of the proton exchange membranes. In order to evaluate the contamination effects of metallic ions dissociated from the bipolar plates on proton exchange membranes during the operation time, the concentrations of metallic ions in the water, which was produced by the operation of the single cell for 100 h, were measured by inductively coupled plasma-mass spectrometer (ICP-MS), and the results are shown in Table 3. The concentrations of Cr, Fe, and Ni ions are 0.1046, 0.148, and 0.104 ppm, respectively. Evidently, the concentrations of metallic ions are very small. In addition, the surface composition of membrane electrode assembly is also examined by the XPS analysis. The binding energy profiles of $Cr_{2P3/2}$, $Fe_{2P3/2}$, and $Ni_{2P3/2}$ are shown in Fig. 11. It is apparently that the concentrations of $Cr_{2P3/2}$ (Fig. 11(a)), $Fe_{2P3/2}$ (Fig. 11(b)), and $Ni_{2P3/2}$ (Fig. 11(c)) on the surface of membrane electrode assembly (MEA) are too small to be detected. Although the contamination of metallic ions in the proton exchange membranes is very little in the testing results, the current efforts on longer testing time of the single cell with the activated-chromized steel bipolar plates are still in progress in our laboratory. The relevant performance and the contaminated effects of metallic ions will be investigated and presented in the future.

4. Conclusions

Three kinds of Fe-based alloys, SS 316, SS 420, and SS 430 steel, treated with rolling and low-temperature pack chromization were evaluated for the application of bipolar plates in PEMFCs. For the same substrate, the rolled-chromized steels exhibited better performance than the simple chromized specimens at the initial stage of cell operation. Above all, the single cell with 420-R-Cr(700-2) bipolar plates showed the highest peak power density of 0.46 W cm^{-2}, which is much close to that of the cell with graphite bipolar plates (0.50 W cm^{-2}), due to the lowest interfacial contact resistance among the chromized steels. In addition, the cell with 420-R-Cr(700-2) bipolar plates exhibited stable current density during the operation of 100 h. The concentrations of Cr, Fe, and Ni in the water produced by the cell with 420-R-Cr(700-2) bipolar plates are lower than 1 ppm. Based on the excellent performance presented above, the rolled-chromized SS 420 steels could be considered as a candidate for bipolar plates in PEMFCs.

References

[1] J. Jayaraj, Y.C. Kim, K.B. Kim, H.K. Seok, E. Fleury, Science and Technology of Advanced Materials 6 (2005) 282–289.
[2] E.A. Choa, U.S. Jeon, S.A. Hong, I.H. Oh, S.G. Kang, Journal of Power Sources 142 (2005) 177–183.
[3] I. Bar-On, R. Kirchain, R. Roth, Journal of Power Sources 109 (2002) 71–75.
[4] J. Wind, R. Spah, W. Kaiser, G. Bohm, Journal of Power Sources 105 (2002) 256–260.
[5] T. Kinumoto, M. Inaba, Y. Nakayama, K. Ogata, R. Umebayashi, A. Tasaka, Y. Iriyama, T. Abe, Z. Ogumi, Journal of Power Sources 158 (2006) 1222–1228.
[6] Y. Wang, D.O. Northwood, Journal of Power Sources 165 (2007) 293–298.
[7] G. Bertrand, H. Mahdjoub, C. Meunier, Surface Coating and Technology 126 (2000) 199–209.
[8] M.P. Brady, K. Weisbrod, I. Paulauskas, R.A. Buchanan, K.L. More, H. Wang, M. Wilson, F. Garzon, L.R. Walker, Scripta Materialia 50 (2004) 1017–1022.
[9] I.E. Paulauskas, M.P. Brady, H.M. Meyer III, R.A. Buchanan, L.R. Walker, Corrosion Science 48 (2006) 3157–3171.
[10] W. Olbrich, J. Fessmann, G. Kampschulte, J. Ebberink, Surface Coating and Technology 49 (1991) 258–262.
[11] C.Y. Bai, T.M. Wen, K.H. Hou, M.D. Ger, Journal of Power Sources 195 (2010) 779–786.
[12] D.P. Davies, P.L. Adcock, M. Turpin, S.J. Rowen, Journal of Power Sources 86 (2000) 237–242.
[13] S.J. Lee, C.H. Huang, J.J. Lai, Y.P. Chen, Journal of Power Sources 131 (2004) 162–168.
[14] H. Wang, M.A. Sweikar, J.A. Turner, Journal of Power Sources 115 (2003) 243–251.
[15] R.F. Silva, D. Franchi, A. Leone, L. Pilloni, A. Masci, A. Pozio, Electrochimica Acta 51 (2006) 3592–3598.
[16] C.Y. Bai, M.D. Ger, M.S. Wu, International Journal of Hydrogen Energy 34 (2009) 6778–6789.
[17] C.H. Hsu, C.F. Chen, H.C. Lo, Thin Solid Films 515 (2006) 1025–1027.
[18] M.P. Brady, H. Wang, B. Yang, J.A. Turner, International Journal of Hydrogen Energy 32 (2007) 3778–3788.
[19] R.J. Tian, J.C. Sun, L. Wang, Journal of Power Sources 163 (2007) 719–724.
[20] Y. Fu, G.Q. Linb, M. Hou, International Journal of Hydrogen Energy 34 (2009) 453–458.
[21] J. Liu, F. Chen, Y.G. Chen, Journal of Power Sources 187 (2009) 500–504.